25th International Meshing Roundtable

Very High Order Anisotropic Metric-Based Mesh Adaptation in 3D

Olivier Coulaud[a], Adrien Loseille[a]

[a]INRIA Saclay-île-de-France, Bâtiment Alan Turing, 91120 Palaiseau, France

Abstract

In this paper, we study the extension of anisotropic metric-based mesh adaptation to the case of very high-order solutions in 3D. This work is based on an extension of the continuous mesh framework and multi-scale mesh adaptation where the optimal metric is derived through a calculus of variations. Based on classical high order *a priori* error estimates, the point-wise leading term of the local error is a homogeneous polynomial of order $k+1$. To derive the leading anisotropic direction and orientations, this polynomial is approximated by a quadratic positive definite form, taken to the power $\frac{k+1}{2}$. From a geometric point of view, this problem is equivalent to finding a maximal volume ellipsoid included in the level set one of the absolute value of the polynomial. This optimization problem is strongly non-linear both for the functional and the constraints. When the discrete problem is considered, the complexity becomes $O(n^6)$ in 3D, where n is the number of nodes used to approximate the level set. We first recast the continuous problem in a discrete setting in the metric-logarithm space. With this approximation, this problem becomes linear and is solved with the simplex algorithm.This optimal quadratic form in the Euclidean space is then found by iteratively solving a sequence of such log-simplex problems. From the field of the local quadratic forms that represents the high-order error, a calculus of variations is used to globally control the error in $\mathbf{L}^p$ norm. A closed form of the optimal metric is then found. Anisotropic meshes are then generated with this metric based on the unit mesh concept. For the numerical experiments, we consider several analytical functions in 3D. Convergence rate and optimality of the meshes are then discussed for interpolation of orders 1 to 5.
© 2016 The Authors. Published by Elsevier Ltd.
Peer-review under responsibility of the organizing committee of IMR 25.

Keywords: Metric-based Mesh Adaptation, High-order interpolation error, Log-Euclidean framework, Log-simplex algorithm, P_k mesh adaptation

Introduction

Anisotropic mesh adaptation has been an active field of research. However, it has been mostly restricted to the case of linear interpolation. Indeed in this case, the interpolation error is expressed in terms of the Hessian of the solution. From a practical point of view, a recovered Hessian is used [15] to derive an optimal metric-field. We have in this case a natural connection between the metric-based generation algorithm and the error estimate [10]. However, when

---

* Corresponding author. Tel.: + 33 1 77 57 80 15.
  E-mail address: Adrien.Loseille@inria.fr

dealing with k order interpolation ($k > 1$), a ($k + 1$) differential form is involved in the analysis [4]. The natural link between the error estimate and the metric-based mesh generation procedure does not exist anymore.

Most of the work to address this issue is done in 2D. One class of techniques consists in approaching the error map (homogeneous polynomial of order $k + 1$) by a metric tensor, see [2,3,9,13]. From a geometric point of view, the problem is equivalent to finding an ellipse of maximal area included in the iso-line of level one of the error. Several improvements are possible by developing $h - p$ method with shock fitting [6,7,14]. However, these methods are hardly applicable numerically in 3D. In [16], an optimization framework is used to predict the behavior of any error systems in 2D and 3D with respect to a change of the metric field. The approach provides a natural coupling with metric-based mesh adaptation. However, the optimal mesh and metric may have a strong dependency on the initial mesh.

In this paper, we consider the 3D case while adopting the geometric point of view. We introduce a new method which can be used for any order of interpolation, even though we restrict the numerical experiments to the order 5. We first recast the continuous problem in a discrete setting in the metric-logarithm space. With this approximation, this problem becomes linear and is solved with the simplex algorithm [5]. This optimal quadratic form in the Euclidean space is then found by iteratively solving a sequence of such log-simplex problems. From the field composed of the local quadratic forms that represents the high-order error, a calculus of variations is used to globally control the error in $\mathbf{L}^p$ norm. A closed form of the optimal metric is then found. This extends the continuous mesh framework and multi-scale metric initially derived for the linear interpolation [10,11] to high order interpolations.

Outline. The paper is organized as follows. In Section 1, we recall the basic notions on interpolation errors and metric-based mesh adaptation that are used in the sequel. In Section 2, we introduce the log-simplex algorithm to derive the local error model of a given initial k-order homogeneous polynomial. We then provide the optimal metric minimizing the k-order interpolation error in $\mathbf{L}^p$ norm. In Section 3, several numerical experiments are discussed for interpolation orders ranging from 1 to 5.

1. Interpolation errors and metric-based mesh adaptation

In this section, we introduce some basic background notions about P_k interpolation and Riemannian metric spaces.

1.1. Polynomial interpolation

We consider the classical Lagrangian interpolation over tetrahedra. For a given tetrahedron $K \subset \mathbb{R}^3$, let $x_1, x_2, ..., x_n$ be a set of points inside K, which we call interpolation nodes. Let Π_k be the projection operator of $C^0(K)$ over the polynomial functions of degree k of K such that for a function u:

$$\Pi_k u(x_i) = u(x_i) \quad \text{for all} \quad i \in \{1, ..., n\}. \tag{1}$$

More precisely, if the interpolation nodes are well chosen, $\Pi_k u$ is the only polynomial of order k satisfying (1). In order to define Π_k well and uniquely, the number of nodes must equal the number of needed coefficients to define a polynomial function of degree k, which is:

$$n = \sum_{i=0}^{k} \sum_{j=0}^{k-i} \sum_{l=0}^{k-i-j} 1 = \sum_{i=0}^{k} \frac{(k + 1 - i)^2 + (k + 1 - i)}{2}.$$

Although we could take these nodes anywhere in K, we have chosen to place them in a uniform way. Let a, b, c and d be the four corners of K and x_i be one of the nodes of K. In the barycentric coordinates with respect to (a, b, c, d), one has $x = (u, v, w, t)$ with $u, v, w, t \in \mathbb{R}$ and $u + v + w + t = 1$. One simple choice consists in considering every combination $(i, j, l, m) \in \mathbb{N}^4$ such that $i + j + l + m = k$ and to define the nodes such that:

$$x = \left(\frac{i}{k}, \frac{j}{k}, \frac{l}{k}, \frac{m}{k} \right) \quad \text{in} \quad (a, b, c, d). \tag{2}$$

In particular, this ensures that the number of nodes defines well the interpolation operator Π_k. Thus, with $\{x_1, ..., x_n\}$ given by (2), Π_k is defined by

$$\Pi_k u(x) = P(x), \text{ for all } x \in K,$$

where P is the polynomial of degree k such that $P(x_i) = u(x_i)$, for all $i \in \{1, ..., n\}$. In what follows, Π_k will denote either the operator on a single tetrahedron and on a mesh composed of several tetrahedra. Notice that there is exactly $k + 1$ nodes on each edge of K and $\frac{k^2+3k+2}{2}$ nodes on each face of K, which are the numbers of nodes needed to define a P_k interpolation operator respectively in one and two dimensions. Consequently, with the choice (2), the operator Π_k preserves the continuousness of a function over the interfaces between tetrahedra. Notice also that another choice of nodes or interpolation would not change the main results of this paper.

From a theoretical point of view, it is well known that the P_k interpolation error of a smooth function u is led by the $(k + 1)$th differential of u, which we note $d^{(k+1)}u$. For instance, for a smooth function u defined on a tetrahedron K, the following inequality holds:

$$\|u - \Pi_k u\|_{L^p(K)} \leq C |K|^{\frac{k+1}{3}} \left\| d^{(k+1)} u \right\|_{L^p(K)}, \tag{3}$$

where $C > 0$, $|K|$ is the volume of K and $\|.\|_{L^p(K)}$ denotes the classical L^p norm on K. The proof of this inequality can be found in a more general case in [4]. The mesh adaptation method that we investigate involves Inequality (3), but consists in replacing the right member of (3) by a 2nd−order term, defined through a well chosen metric field $\mathcal{M}$:

$$\|u - \Pi_k u\|_{L^p(K)} \leq C |K|^{\frac{k+1}{3}} \| \mathcal{M} \|_{L^p(K)}^{\frac{k+1}{2}}. \tag{4}$$

This choice is motivated by the need and the capacity of generating anisotropic meshes by using the metric-based approach and unit-mesh concept.

1.2. Metric-based mesh adaptation

In this section, we recall the theoretical background of metric-based anisotropic mesh adaptation. It is closely related to Riemannian geometry, and we refer to [10,11] for further details about these notions. In what follows, $\mathcal{M}$ denotes a metric of $\mathbb{R}^3$, a symmetric positive definite matrix.

Definition 1.1. *An Euclidean metric space* $(\mathbb{R}^3, \mathcal{M})$ *is a finite vector space where the dot product is defined by means of a metric* $\mathcal{M}$. *More precisely, we set* $\langle u, v \rangle_{\mathcal{M}} = {}^t u \mathcal{M} v$, *for* $u, v \in \mathbb{R}^3$. *Since* $\mathcal{M}$ *is symmetric, positive and definite, the product* $\langle ., . \rangle_{\mathcal{M}}$ *is a scalar product on* $\mathbb{R}^3$. *The norm* $\|.\|_{\mathcal{M}}$ *results from this scalar product and is given by* $\|u\|_{\mathcal{M}} = \sqrt{{}^t u \mathcal{M} u}$, *for all* $u \in \mathbb{R}^3$.

From a geometric point of view, in the space $(\mathbb{R}^3, \mathcal{M})$ the unit ball $\mathcal{B}_{\mathcal{M}}$ of $\mathcal{M}$ is the sphere of radius 1. On the other hand, in the Euclidean space, $\mathcal{B}_{\mathcal{M}}$ is an ellipsoid defined through the positive eigenvalues $\{\lambda_1, \lambda_2, \lambda_3\}$ and eigenvectors $\{v_1, v_2, v_3\}$ of $\mathcal{M}$. Let $h_i = \frac{1}{\sqrt{\lambda_i}}$, $i = 1, ..., 3$ be the principal lengths of $\mathcal{M}$. The metric can be written $\mathcal{M} = R \Lambda {}^t R$, with

$$R = (v_1 \,|\, v_2 \,|\, v_3) \quad \text{and} \quad \Lambda = \begin{pmatrix} \frac{1}{h_1^2} & 0 & 0 \\ 0 & \frac{1}{h_2^2} & 0 \\ 0 & 0 & \frac{1}{h_3^2} \end{pmatrix}.$$

Working in an Euclidean metric space $(\mathbb{R}^3, \mathcal{M})$ actually reduces to applying the mapping $\mathcal{M}^{\frac{1}{2}} = {}^t R \sqrt{\Lambda} R$ to $\mathbb{R}^3$. For later use, for $s \in \mathbb{R}$, we also define $\mathcal{M}^s = {}^t R \Lambda^s R$, where Λ^s is obtained by replacing λ_i by λ_i^s, for $i = 1, 2, 3$.

Let us now consider the case where the metric tensor is not constant over Ω. $\mathbf{M} = (\mathcal{M}(x))_{x \in \Omega}$ denotes a continuous metric tensor. Following the definitions related to the classical Euclidean metric spaces, one can define the length between two points $a, b \in \mathbb{R}^3$ with respect to $\mathbf{M}$. Let $\gamma(t) = a + t\,ab$ with $t \in [0, 1]$ be the parametrization of the segment ab. The length $\ell(ab)$ of ab is then given by

$$\ell(ab) = \int_0^1 \|\gamma'(t)\|_{\mathcal{M}} \, dt = \int_0^1 \sqrt{{}^t ab \, \mathcal{M}(\gamma(t)) \, ab} \, dt.$$

From this formula, one can now state the notion of unit mesh with respect to a continuous metric. The following definition establishes a relation between a metric field and a mesh.

Definition 1.2. *A tetrahedron K is unit with respect to a metric* $\mathbf{M}$ *if the lengths of its edges equal* 1 *in the metric* $\mathbf{M}$. *If* $(e_i)_{i=1,...,6}$ *are the edges of K, one has* $\ell_{\mathcal{M}}(e_i) = 1$, *for all* $i \in \{1, ..., 6\}$.

From this definition, it is clear that there is an analogy between a mesh and a metric field, as far as there is an analogy between a tetrahedron and a metric. Indeed, one can express some classical notions concerning meshes in terms of continuous metric field. For instance, in the case of a constant metric $\mathcal{M}$, the volume of a unit element K equals $|K| = \frac{\sqrt{2}}{12} \det\left(\mathcal{M}^{-\frac{1}{2}}\right)$. Consequently, in the case of a continuous metric field, the volume of an element K can be linked to the volume of the unit ball of $\mathcal{M}(x)$, which is

$$\left|\mathcal{B}_{\mathcal{M}(x)}\right| = \frac{4\pi}{3} \det\left(\mathcal{M}(x)\right)^{-\frac{1}{2}}.$$

Likewise, the complexity, which is the counterpart of the number of vertices of a mesh, can be now defined as the quantity:

$$C(\mathbf{M}) = \int_{\Omega} \sqrt{\det \mathcal{M}(x)} \, dx.$$

Indeed, if $C(\mathbf{M})$ is large, the volumes of the units balls of $\mathbf{M}$ are small. This definition has the same meaning as the classical notion of complexity in the case of a mesh, where a large complexity implies tetrahedra with small volumes. In the following, the complexity is used as the main parameter to govern the desired accuracy.

2. High order error model

In this section, we describe the error model and the optimisation method that we use to approximate $d^{(k+1)}u$. For $u \in C^{k+1}(\Omega)$ and $x_0 \in \Omega$, one has, for all $x \in \Omega$:

$$|u(x) - \Pi_k u(x)| \leq C \left|d^{(k+1)}u(x_0)(x - x_0)\right| + o\left(\|x - x_0\|_2^{k+1}\right), \tag{5}$$

where C is a positive constant. In this inequality, we recall that $d^{(k+1)}u(x_0)$ is a homogeneous polynomial function of degree $k + 1$. The main idea to control the interpolation error consists in finding a metric field $\mathbf{Q} = (Q(x))_{x \in \Omega}$ such that:

$$\left|d^{(k+1)}u(x)(y)\right| \leq \left|{}^t y \, Q(x) \, y\right|^{\frac{k+1}{2}}, \quad \text{for all} \quad x \in \Omega, y \in \mathbb{R}^3. \tag{6}$$

Once $\mathbf{Q}$ is found, one can deduce an optimal metric field $\mathbf{M}$ which minimizes the interpolation error, like in the case of the P_1 interpolation. In order to be as close as possible to the equality in (6), the volume of the unit ball of $Q(x)$ must be as large as possible, which is equivalent to consider that $\det(Q(x))$ is minimal, for all $x \in \Omega$. Consequently, from a homogeneous polynomial p of degree $k + 1$, which stands for $d^{(k+1)}u$, the problem can be reduced to finding a metric Q such that:

$$\begin{cases} \det Q \text{ is minimal,} \\ |p(x)| = 1 \implies {}^t x \, Q \, x \geq 1. \end{cases} \tag{7}$$

Indeed, since p is a homogeneous polynomial of degree $k+1$, if Q satisfies the second line of (7) for a point $x \in \mathbb{R}^3 \backslash \{0\}$, then we have $\left|p\left(\dfrac{x}{p(x)^{\frac{1}{k+1}}}\right)\right| = 1$, and thus:

$$\left(\frac{{}^t x \, Q \, x}{p(x)^{\frac{2}{k+1}}}\right)^{\frac{k+1}{2}} \geq 1 \quad \Longleftrightarrow \quad \left({}^t x \, Q \, x\right)^{\frac{k+1}{2}} \geq |p(x)|.$$

The initial condition (6) is verified. From a geometric point of view, we seek for the largest ellipsoid contained in the level curve of p of level 1, see Figure 1.

For the linear case ($k = 1$), Q is simply the absolute Hessian of u, $|H_u|$. For higher interpolates, the main difficulty is then to derive an optimal metric verifying (7). To do so, we devise a log-simplex algorithm.
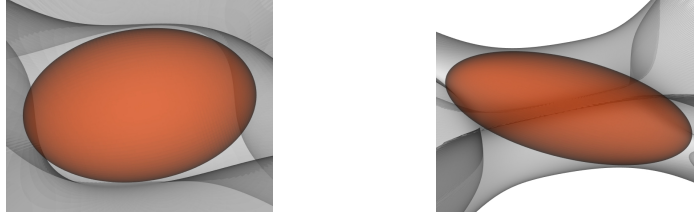
Fig. 1. Example of embedded ellipsoids (in red) into polynomial level curves (in grey) verifying the geometric inequality (6).

2.1. The log-simplex problem

Numerically, we do not consider the entire level curve of P of value 1 but only a few points on it. Let $\{x_1, ..., x_n\}$ be a set of points such that $|p(x_i)| = 1$, for all $i = 1, ..., n$. The continuous problem (7) is thus replaced by the discrete one

$$\begin{cases} \det(Q) & \text{is minimal,} \\ {}^t x_i \, Q \, x_i \geq 1, & \text{for all} \quad i \in \{1, ..., n\} \, . \end{cases} \qquad (8)$$

Unfortunately, this problem is always ill-posed, since we can build an ellipsoid passing between two points, with arbitrary long principal length, which makes the determinant of Q converging to 0, or equivalently the volume of $\mathcal{B}_Q$ going to infinity.
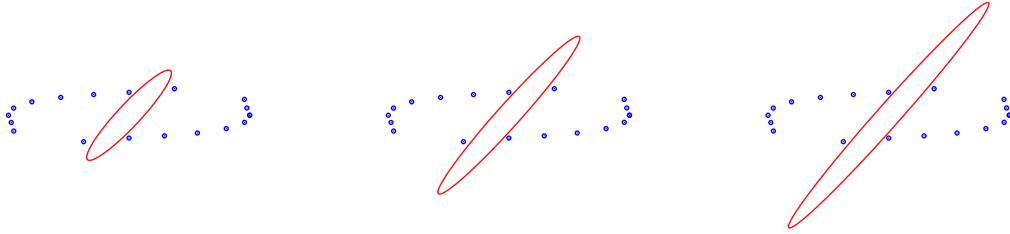

Fig. 2. Sequence of diverging metrics, embedded into a set of points representing an error curve when solving direclty (8).

To overcome this difficulty, we propose another approach, which transforms the non-linear ill-posed optimisation problem (8) into a well-posed linear one. For a metric $Q = R\Lambda^t R$, we define $\mathcal{L} = \log(Q)$ the symmetric matrix given by:

$$\mathcal{L} = R \begin{pmatrix} \log(\lambda_1) & 0 & 0 \\ 0 & \log(\lambda_2) & 0 \\ 0 & 0 & \log(\lambda_3) \end{pmatrix} {}^t R,$$

where $\{\lambda_1, \lambda_2, \lambda_3\}$ are the eigenvalues of Q. Notice that $\mathcal{L}$ is no longer a metric, since it is generally neither positive nor definite. One of the ideas that is largely used in this paper is to consider an optimisation problem for $\mathcal{L}$ instead of Q itself. One property of $\log(Q)$ that we will take advantage is that $\det(Q) = \exp(\mathrm{trace}(\mathcal{L}))$. As a consequence, the non-linear cost function $Q \to \det(Q)$ of Problem (8) can be changed into the linear one $\mathcal{L} \to \mathrm{trace}(\mathcal{L})$. On the contrary, the conditions ${}^t x_i \, Q \, x_i \geq 1$ which are linear in Q are replaced by ${}^t x_i \exp(\mathcal{L}) x_i \geq 1$, which are strongly non-linear in $\mathcal{L}$. One of the main ideas of this paper is to modify the conditions on $\mathcal{L}$ into approximated linear conditions.

Let $x \in \mathbb{R}^3 \setminus \{0\}$ such that ${}^t x Q x \geq 1$. Making the change of variables $\tilde{x} = {}^t R x$ and setting $\{\mu_1, \mu_2, \mu_3\}$ the eigenvalues of $\mathcal{L}$, we have:

$$ {}^t x \exp(\mathcal{L}) x \geq 1 \iff \sum_{j=1}^{3} \exp(\mu_j) \tilde{x}_j^2 \geq 1 \iff \sum_{j=1}^{3} \exp(\mu_j) \frac{\tilde{x}_j^2}{\|\tilde{x}\|_2^2} \geq \frac{1}{\|\tilde{x}\|_2^2}, $$

where $\|\tilde{x}\|_2$ is the Euclidean norm of $\tilde{x}$. In particular, it is clear that $\sum_{j=1}^{3} \dfrac{\tilde{x}_j^2}{\|\tilde{x}\|_2^2} = 1$, and since R is a rotation matrix one has $\|\tilde{x}\|_2 = \|x\|_2$. Consequently, the convexity of the exponential gives:

$$\sum_{j=1}^{3} \exp(\mu_j) \frac{\tilde{x}_j^2}{\|\tilde{x}\|_2^2} \geq \exp\left(\sum_{j=1}^{3} \mu_j \frac{\tilde{x}_j^2}{\|\tilde{x}\|_2^2}\right) = \exp\left(\frac{{}^t x \mathcal{L} x}{\|x\|_2^2}\right).$$

Thus, we can replace the second line of (8) by the approximated condition:

$$ {}^t x \mathcal{L} x \geq -\|x\|_2^2 \log\left(\|x\|_2^2\right), $$

which is now linear in $\mathcal{L}$.

Finally, the optimisation problem that we consider is the following:

Find a symmetric matrix $\mathcal{L}$ such that

$$\begin{cases} \text{trace}(\mathcal{L}) \quad \text{is minimal}, \\ {}^t x_i \mathcal{L} x_i \geq -\|x_i\|_2^2 \log\left(\|x_i\|_2^2\right), \quad \text{for all} \quad i \in \{1, ..., n\}. \end{cases} \tag{9}$$

This is actually well-posed, in the sense that the trace of $\mathcal{L}$ cannot go to $-\infty$, which implies that the determinant of Q cannot go to 0 and equivalently that the volume of $\mathcal{B}_Q$ is bounded. This is stated in the next proposition.

Proposition 2.1. *Let $\mathcal{L}$ be a symmetric matrix of $\mathbb{R}^n$, with $n = 2, 3$. Assume that there exist n points $x_1, ..., x_n \in \mathbb{R}^n$ such that:*

$$ {}^t x_i \mathcal{L} x_i \geq -\|x_i\|_2^2 \log\left(\|x_i\|_2^2\right), \quad \text{for all} \quad i \in \{1, ..., n\}. \tag{10}$$

If $(x_1, ..., x_n)$ is an orthogonal basis of $\mathbb{R}^n$, then there exists a constant $C \in \mathbb{R}$ such that:

$$ \text{trace}\left(\mathcal{L}\right) \geq C. $$

Proof: The proof of this proposition is done in 2D, but the extension to 3D is straightforward. Let $\mathcal{L}$ be a symmetric matrix of $\mathbb{R}^2$. We write:

$$ \mathcal{L} = \begin{pmatrix} a & c \\ c & b \end{pmatrix}, \text{ with } a, b, c \in \mathbb{R}. $$

Let (x_1, x_2) be an orthogonal basis of $\mathbb{R}^2$ satisfying (10). Up to a rotation, one assumes that $x_1 = (r_1, 0)$ and $x_2 = (0, r_2)$ with $r_1, r_2 > 0$. The assumption (10) reads:

$$\begin{aligned} a r_1^2 &\geq -r_1^2 \log(r_1^2), \\ b r_2^2 &\geq -r_2^2 \log(r_2^2). \end{aligned} \quad \Longleftrightarrow \quad \begin{aligned} a &\geq -\log(r_1^2), \\ b &\geq -\log(r_2^2). \end{aligned}$$

Consequently, we deduce:

$$ \text{trace}\left(\mathcal{L}\right) = a + b \geq -\left(\log(r_1^2) + \log(r_2^2)\right), $$

which achieves the proof of this proposition.

$\square$

We have reduced the problem (8) which is non-linear and ill-posed into (9), which is linear and well-posed under linear constraints. We will see in the next section that, by approximating the constraints through the convexity of the exponential, this problem can be far from the initial one, but an iterative process enables to make it converge to the initial one.

The resolution of (9) is done by the simplex algorithm. Indeed, the matrix $\mathcal{L}$ can be viewed as a vector $w_Q = (a, b, c, d, e, f)$ of $\mathbb{R}^6$,

$$\mathcal{L} = \begin{pmatrix} a & b & c \\ b & d & e \\ c & e & f \end{pmatrix}.$$

For each $i \in \{1, ..., n\}$, x_i denotes both a point of $\mathbb{R}^3$ and its coordinates (x_i, y_i, z_i). The log-simplex problem (9) can be rewritten:

$$\begin{cases} \text{minimize} \quad a + d + f, \\ x_i^2 a + 2x_i y_i b + 2x_i y_i c + y_i^2 d + 2y_i z_i e + f z_i^2 \geq C_i, \quad \text{for all} \quad i = 1, ..., n, \end{cases}$$

with $C_i = -\|x_i\|_2^2 \log\left(\|x_i\|_2^2\right)$. With this formalism, each constraint corresponds to an hyperplane of $\mathbb{R}^6$, and the whole set of constraints forms a simplex in $\mathbb{R}^6$ in which the admissible solutions are taken. The cost function is nothing more than $\langle v, w_Q \rangle_{\mathbb{R}^6}$ with $v = (1, 0, 0, 1, 0, 1)$. This illustrates that the direction $-v$ prevails among the others to make the cost function decrease. In particular, if there is an optimal admissible solution, it must be a node at the intersection of six hyperplanes. More details on the numerical implementation of the simplex algorithm can be found in [5].

2.2. Resolution of the log-simplex problem

With the simplex algorithm, we are able to solve the log-simplex problem. But, since we make the convex approximation (9) on the constraints, it is not always sufficient to obtain an accurate metric Q. Indeed, as we can see on Figure 2.2, the log-constraints can be far from the initial ones when the level set of p is anisotropic.
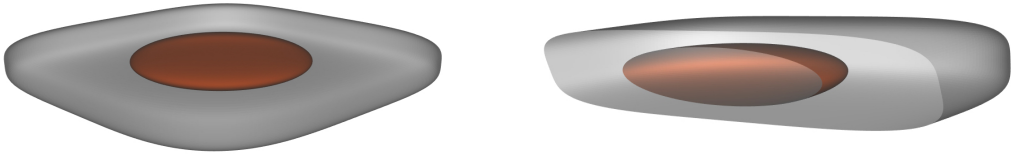

Fig. 3. Illustration of the log approximation for the constraints for an error level 1 (in grey). The log-simplex optimal metric (in red) is far from the boundary of the error due to the convexity approximation.

To avoid this problem, we consider an iterative process. The idea is to perform iteratively the change of variable $\tilde{x} = Q^{\frac{1}{2}} x$ on $\mathbb{R}^3$. By doing this, we transform the ellipsoid $\mathcal{B}_Q$ into the sphere $S^2 \subset \mathbb{R}^3$. We then perform the simplex method with a set of points chosen on the level set of level 1 of $p \circ Q^{-\frac{1}{2}}$ and iterate the process, which gives a sequence $(Q_j)_{j \in \mathbb{N}}$ of metrics.

More precisely, let $\{z_1, ..., z_n\}$ be a set of points of the unit sphere $S^2 \in \mathbb{R}^3$. Given a metric Q_j, we obtain a set of points $\{y_1, ..., y_n\}$ of the level set of $p \circ Q_j^{-\frac{1}{2}}$ through the mapping :

$$y_i = \frac{z_i}{\left| p(Q_j^{-\frac{1}{2}} z_i) \right|^{\frac{1}{k}}}.$$

Then, we perform the log-simplex algorithm and solve the problem (9) with the constraints points $(y_i)_{i=1,...,n}$ and obtain an optimal symmetric matrix $\mathcal{L}_{j+1}$. Finally, we recover Q_{j+1} in the original variables by the formula :

$$Q_{j+1} = Q_j^{\frac{1}{2}} \exp\left(\mathcal{L}_{j+1}\right) Q_j^{\frac{1}{2}}.$$

The next theorem ensures that if this iterative process converges to a metric Q, then this metric approximates well the level set of level 1 of p.

Theorem 2.1. *Let p be a homogeneous polynomial and $\{z_1, ..., z_n\}$ be a set of points of $\mathbb{R}^3$ such that $\|z_i\|_2 = 1$ for all $i = 1, ..., n$. Let $(Q_j)_{j \in \mathbb{N}}$ be the sequence of metrics of $\mathbb{R}^3$ defined by*

- $Q_0 = I_3$
- $Q_j = Q_{j-1}^{\frac{1}{2}} \exp\left(\mathcal{L}_j\right) Q_{j-1}^{\frac{1}{2}}$ *where* $\mathcal{L}_j$ *is an optimal solution of the log-simplex* (9) *problem with the constraint points* $\{y_1^j, ..., y_n^j\}$ *defined by:*

$$y_i^j = \frac{z_i}{\left| p(Q_{j-1}^{-\frac{1}{2}} z_i) \right|^{\frac{1}{k}}}, \text{ for all } i = 1, ..., n.$$

If the sequence $(Q_j)_{j \in \mathbb{N}}$ *converges to a metric* Q *then the sequence* $(y_i^j)_{j \in \mathbb{N}}$ *converges to* $y_i \in \mathbb{R}^3$, $(\mathcal{L}_j)_{j \in \mathbb{N}}$ *converges to* $\mathcal{L} = 0$. *Furthermore, we have:*

$${}^t y_i \, \mathcal{L} \, y_i \geq - \|y_i\|_2^2 \log\left(\|y_i\|_2^2\right) \quad \Longleftrightarrow \quad {}^t x_i \, Q \, x_i \geq 1,$$

where, for all $i \in \{1, ..., n\}$, $x_i = Q^{-\frac{1}{2}} y_i$ *is a point of the level set of level* 1 *of* p.

Proof: The proof of this theorem is almost straightforward. Assume that $Q_j \rightarrow Q$ when j goes to infinity. Since

$$\mathcal{L}_j = \log\left(Q_{j-1}^{-\frac{1}{2}} Q_j Q_{j-1}^{-\frac{1}{2}}\right),$$

by passing to the limit when $j \rightarrow +\infty$, we deduce that $\mathcal{L}_j$ converges to a symmetric matrix $\mathcal{L} = \log(I_3) = 0$. It is also clear that, since $(z_i)_{i=1,...n}$ is fixed, y_i^j converges for every i to $y_i = \dfrac{z_i}{p(Q^{-\frac{1}{2}} z_i)^{\frac{1}{k}}}$ when $j \rightarrow +\infty$. By passing to the limit in the constraint inequalities of (9), we get:

$$0 \geq - \|y_i\|_2^2 \log\left(\|y_i\|_2^2\right) \Longleftrightarrow 0 \geq - \frac{1}{\left| p(Q^{-\frac{1}{2}} z_i) \right|^{\frac{2}{k}}} \log\left(\frac{1}{\left| p(Q^{-\frac{1}{2}} z_i) \right|^{\frac{2}{k}}} \right) \Longleftrightarrow 0 \geq \log\left(\left| p(Q^{-\frac{1}{2}} z_i) \right|^{\frac{2}{k}} \right) \Longleftrightarrow 1 \geq \left| p(Q^{-\frac{1}{2}} z_i) \right|^{\frac{2}{k}}.$$

Since, $\|z_i\|_2 = {}^t z_i \, Q^{-\frac{1}{2}} \, Q \, Q^{-\frac{1}{2}} \, z_i = 1$, we have:

$$\frac{1}{\left| p(Q^{-\frac{1}{2}} z_i) \right|^{\frac{2}{k}}} \geq 1 \Longleftrightarrow \frac{{}^t z_i \, Q^{-\frac{1}{2}} \, Q \, Q^{-\frac{1}{2}} \, z_i}{\left| p(Q^{-\frac{1}{2}} z_i) \right|^{\frac{2}{k}}} \geq 1 \Longleftrightarrow {}^t \left(\frac{Q^{-\frac{1}{2}} z_i}{\left| p(Q^{-\frac{1}{2}} z_i) \right|^{\frac{1}{k}}} \right) Q \left(\frac{Q^{-\frac{1}{2}} z_i}{\left| p(Q^{-\frac{1}{2}} z_i) \right|^{\frac{1}{k}}} \right) \geq 1 \Longleftrightarrow {}^t x_i \, Q \, x_i \geq 1,$$

which achieves the proof.

$\square$

2.3. Infinite branches

Another difficulty lies in the fact that the level set 1 of the homogeneous polynomial p can have infinite branches, *i.e.*, sub vector spaces such that for a non-zero vector $x_0 \in \mathbb{R}^3$, we have $p(x_0) = 0$. In this case, the log-simplex algorithm can produce a sequence of metrics $(Q_j)_{j \in \mathbb{N}}$ such that $\det(Q_j) \rightarrow 0$ when j goes to infinity, or equivalently the volume of the unit ball of Q_j goes to infinity.
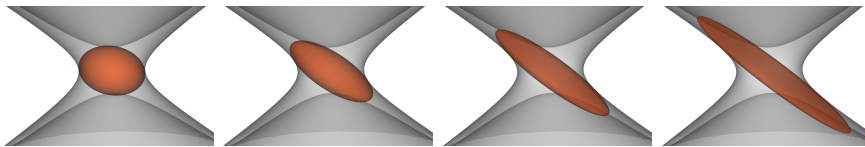

Fig. 4. Grey: the level set of a polynomial of degree 2. Red: a sequence of metrics whose volume go to infinity

The strategy to get rid of those infinite branches is based on the factorization of the polynomial p to an approximated version of it which does not have vanishing points. Notice that in the case of the P_1 interpolation, this problem does not occur, since we only have to take $Q = |H_u|$, with H_u the Hessian matrix of u. We take advantage of the next proposition.

Proposition 2.2. *Let p be a homogeneous polynomial of degree d given by*

$$p(x, y, z) = \sum_{i+j+k=d} a_{i,j,k} \binom{d}{i, j, k} x^i y^j z^k, \quad where \quad a_{i,j,k} \in \mathbb{R} \quad and \quad \binom{d}{i, j, k} = \frac{d!}{i! j! k!}.$$

The polynomial p can be written:

$$p(x, y, z) = \sum_{i+j+k=d-2} x^i y^j z^k \left({}^t X H_{ijk} X \right),$$

where $X = (x, y, z)$ and $(H_{i,j,k})_{i+j+k=d-2}$ are explicit symmetric matrices given by

$$H_{ijk} = \begin{pmatrix} a_{i+2,j,k} & 2a_{i+1,j+1,k} & 2a_{i+1,j,k+1} \\ 2a_{i+1,j+1,k} & a_{i,j+2,k} & 2a_{i,j+1,k+1} \\ 2a_{i+1,j,k+1} & 2a_{i,j+1,k+1} & a_{i,j,k+2} \end{pmatrix}$$

Proof: This proposition is due to H. Borouchaki and P-L. George [1]. The proof is straightforward.

$\square$

When resolving the log-simplex problem, one replaces the homogeneous polynomial p of order $k + 1$ by the function

$$q(x, y, z) = \sum_{i+j+l=k-1} \left| x^i y^j z^l \right| \left({}^t X \left| H_{ijl} \right| X \right),$$

where k is the interpolation order and $(H_{i,j,l})_{i+j+l=k-1}$ is given by Proposition 2.2. Through this method, we are able to avoid infinite branches in the resolution of the log-simplex problem.

2.4. Optimal multi-scale metric

Once we have computed the metric field $\mathbf{Q} = (Q(x))_{x \in \Omega}$, we then have to derive the optimal metric field $\mathbf{M_{L^p}} = (\mathcal{M}_{L^p}(x))_{x \in \Omega}$ which minimizes the L^p−interpolation error when considering unit meshes with respect to $\mathbf{M_{L^p}}$. To do so, we follow the steps developed in [11]. In our case, we can show that for all $\mathcal{H}$ unit mesh with respect to a metric field $\mathbf{M} = (\mathcal{M}(x))_{x \in \Omega}$ with fixed complexity N, there exists a positive constant C such that:

$$\|u - \Pi_k u\|_{\mathcal{H}, L^p} \leq C \left(\int_\Omega \left| \text{trace} \left(\mathcal{M}^{-\frac{1}{2}}(x) Q(x) \mathcal{M}^{-\frac{1}{2}}(x) \right) \right|^{\frac{p(k+1)}{2}} dx \right)^{\frac{1}{p}} = E_{L^p}(\mathbf{M}). \tag{11}$$

Then, by a calculus of variations that we solve by following [11], we obtain the optimal metric field $\mathbf{M_{L^p}}$ which minimizes the right hand side of the inequality (11). It is given by

$$\mathcal{M}_{\mathbf{L^p}} = N^{\frac{2}{3}} \left(\int_\Omega (\det Q)^{\frac{p(k+1)}{2p(k+1)+6}} \right)^{-\frac{2}{3}} (\det Q)^{\frac{-1}{p(k+1)+3}} Q,$$

and satisfies the following equality:

$$E_{\mathbf{L^p}}(\mathbf{M_{L^p}}) = 3^{\frac{k+1}{p(k+1)+6}} N^{-\frac{k+1}{3}} \left(\int_\Omega Q^{\frac{p(k+1)}{2p(k+1)+6}} \right)^{\frac{p(k+1)+3}{3p}}.$$

In particular, if $k = 1$ and $Q = H_u$, one recovers the optimal metric obtained for the P_1 adaptation. Notice also that theoretically, one obtains the following asymptotic rate of convergence

$$E_{\mathbf{L^p}}(\mathbf{M_{L^p}}) = O\left(\frac{1}{N^{\frac{k+1}{3}}} \right) \quad \text{when} \quad N \to +\infty. \tag{12}$$

3. Numerical simulations

For the numerical validations, the adaptive strategy is illustrated for interpolations of order 1 to 5. For each function, only the discrete P_k solution is used to recover the differential form of order $k + 1$., *i.e.*, we never used the exact derivatives of the function, only its point-wise values are used. To do so, we have extended the $\mathbf{L}^2$ projection to the case of high-order differential forms [15]. Once the numerical $(k + 1)$ differential form is recovered, we apply the log-simplex algorithm and derive the optimal $\mathbf{L}^p$ metric for a given complexity. The interpolation error $\|u - \Pi_k u\|_{\mathbf{L}^2(\Omega)}$ is computed using a 10th order Gauss quadrature integration. To compare simultaneously different interpolation orders, the degrees of freedom (DoF) are used instead of the number of the nodes. The error is then used to compare the convergence rate to the optimal one (12). We also compare the interpolation error with respect to sequences of uniform meshes. The anisotropic meshes are generated by using a unique cavity operator [12]. We now describe the analytical functions.

The first function g is derived from the gyroid equation:

$$g(x, y, z) = 10\left(500\cos(x)\sin(y) + 50\cos(y)\sin(z) + 10\cos(z)\sin(x)\right)$$
$$-2\left(\cos(x)\cos(y) + 0.5\cos(y)\cos(z) + \cos(z)\cos(x)\right) - 10.$$

This function is very smooth. The iso-values are depicted in Figure 5 (left). For interpolation of order k with $k \in [1, 5]$ the asymptotic convergence order $k + 1$ is reached very quickly for each k, see Figure 5 (middle). The finest P_1 mesh is composed of 606 834 vertices, 83 338 triangles and 3 536 090 tetrahedra. For an equivalent level of DoF, the P_2 mesh is composed of 68 578 vertices, 15 274 triangles and 390 385 tetrahedra, the P_3 of 17 263 vertices, 5 606 triangles and 95 359 tetrahedra, the P_4 8 755 vertices 3 432 triangles and 47 348 tetrahedra and the P_5 of 4 502 vertices, 2 218 triangles and 23 519 tetrahedra, see Figure 6. Due to the high-regularity of the function, the level of anisotropy decreased when k increases. To assess the optimality of the meshes, the comparison with the error obtained on uniform mesh is depicted in Figure 5 (right). For each k, the adapted meshes are always below the error curves of the uniform meshes.
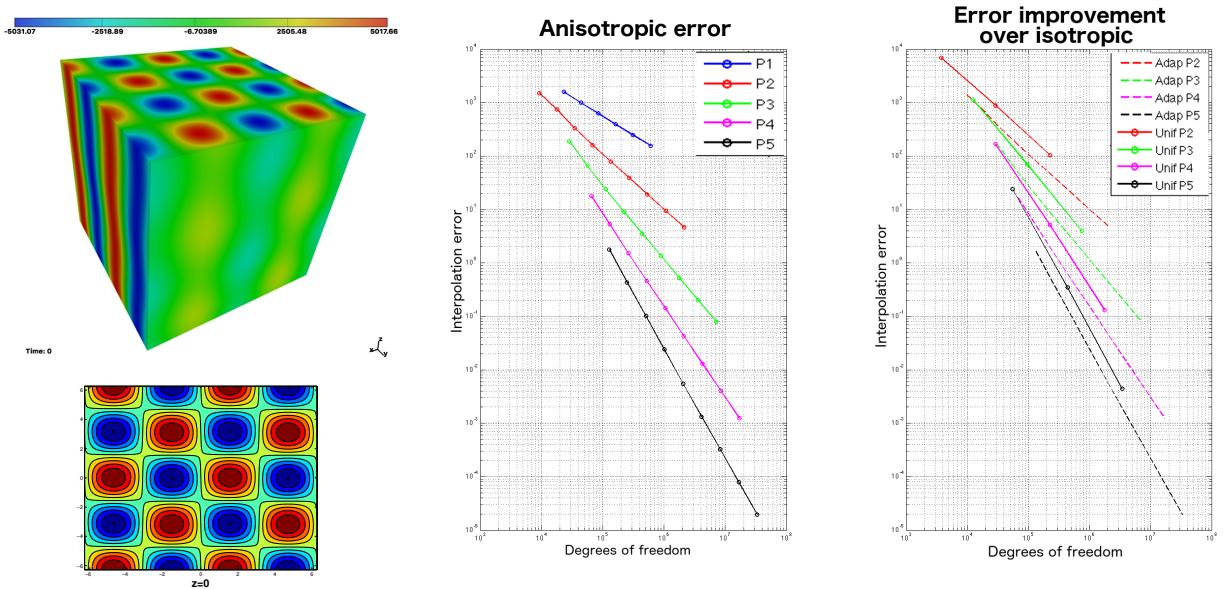

Fig. 5. From left to right, gyroid function g iso-values, rate of convergence for the optimal meshes for order 1,2,3,4 and 5 and comparaison with uniform meshes. Uniform meshes correspond to plain lines while adapted meshes to dashed lines. The same color corresponds to the same interpolation order.

The second function oscillates at high frequency and contains small details, it is given by :

$$f_r(x, y, z) = 8\, xyz\, \sin(5\pi\, xyz)^4 + \frac{1}{10}\left(1 - (\sin(5\pi\, xyz)^4)\right)^8 \cos(100\pi\, xyz). \tag{13}$$
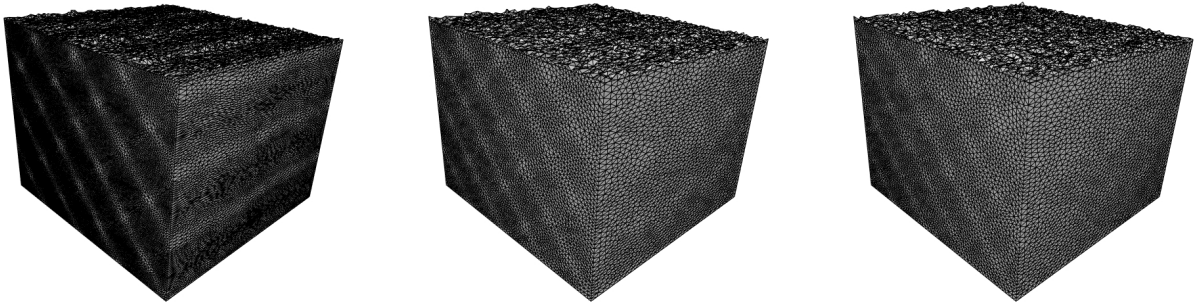
Fig. 6. P_1, P_3 and P_5 meshes for an equivalent level of DoF.

The high frequencies variations of the function is depicted in Figure 7 (left). In this case, the asymptotic rate of convergence is not reached directly due to the small details of the function that are captured for sufficiently small sizes of the mesh, especially for $k > 1$. This does not appear for the linear case as the finest mesh is still too coarse with respect to these variations of small amplitudes. The final mesh for P_1 contains more that 2 000 000 vertices while the equivalent mesh for P_5 in term of DoF contains 19 779 vertices, 11 214 triangles and 101 592 tetrahedra for a error level 3 orders of magnitude below the linear curve. The uniform meshes have a similar behavior, see Figure 7 (right). Again, the sequence of adaptive meshes have lower error curves and the error is 2 order of magnitude smaller in the asymptotic range for P_5 interpolation. Contrary to the gyroid function, a high level of anisotropy is kept for all k due to the small frequencies, see Figure 8.
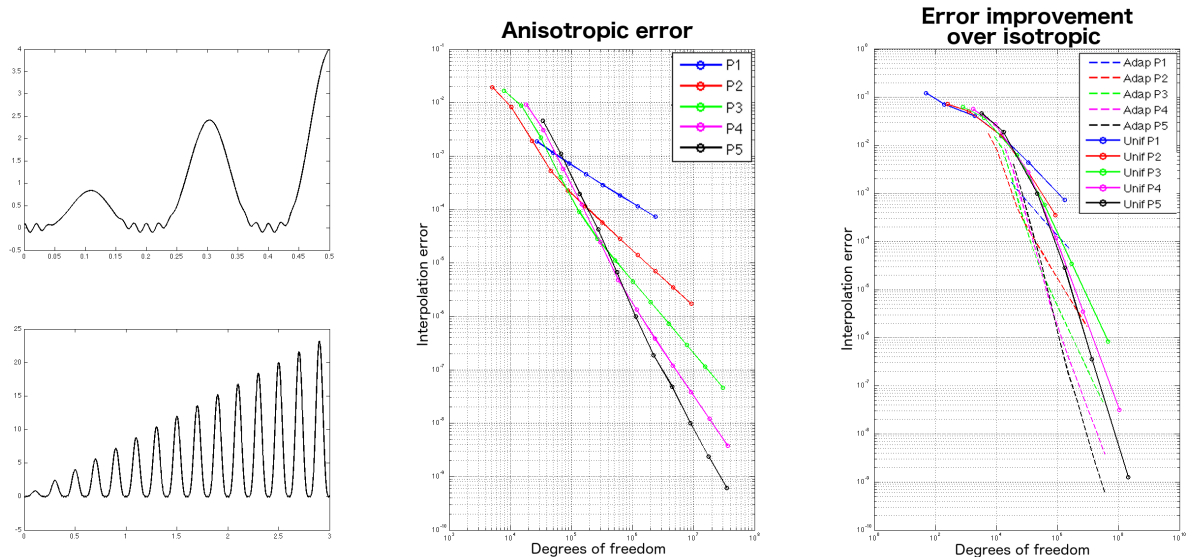

Fig. 7. From left to right, 1D extraction along the line $xyz = cst$, rate of convergence for the optimal meshes for order 1,2,3,4 and 5 and comparisons with uniform meshes. Uniform mesh correspond to plain lines while adapted meshes to dashed lines. The same color corresponds to the same interpolation order.

The last function represents a smooth shock function:

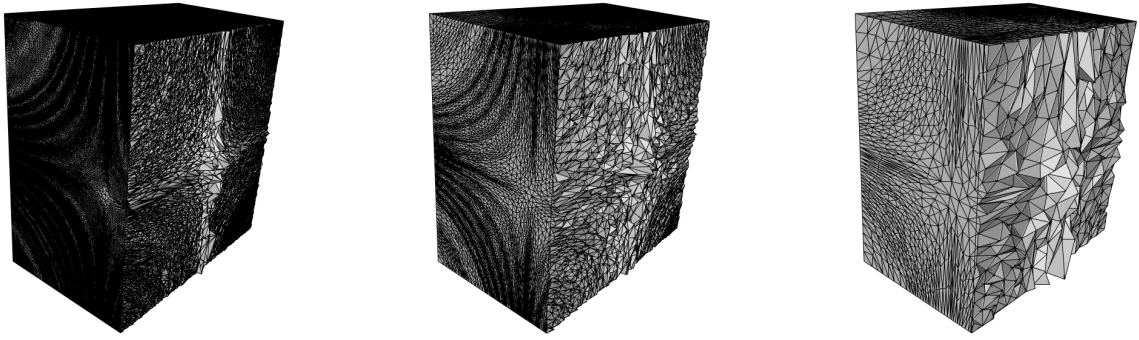$$f_s(x, y, z) = 10\,\mathrm{atan}\left(\frac{x}{\epsilon}\right) + \cos(y\,z) \text{ with } \epsilon = 0.01.$$

Fig. 8. P_1, P_2 and P_4 adapted meshes respectively for the same number of DoF for f_r function.

In this case, the asymptotic rate of convergence is reached for larger DoF for $k = 3, 4, 5$ due to the Gibbs phenomena that occur on small complexity (coarse) meshes. The most interesting feature is to see that the asymptotic rate of convergence is not reached for practical sizes in the case of uniform meshes, see Figure 9 (right) whereas this order is captured far earlier with adaptivity. For P_5, almost we have 10 order of magnitudes gain for the adaptive mesh with respect to the uniform one. For the first 3 meshes for $k = 3, 4, 5$, the meshes are extremely coarse, less than 3 000 nodes.
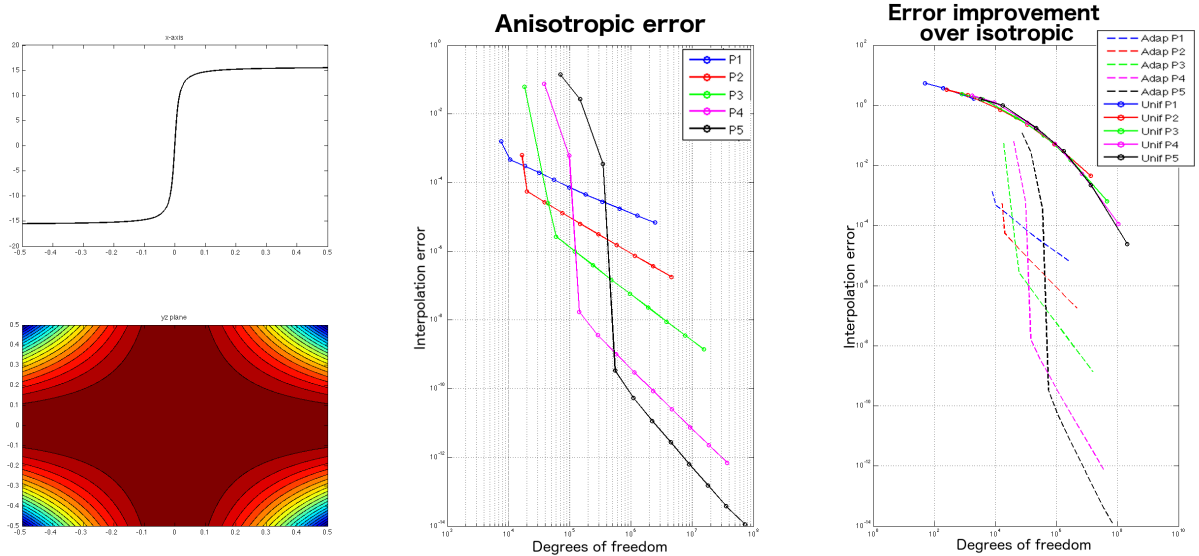

Fig. 9. From left to right, 1D extraction along x-axis, and iso-values in *yz*-axes, rate of convergence for the optimal meshes for order 1,2,3,4 and 5 and comparison with uniform meshes. Uniform meshes correspond to plain lines while adapted meshes to dashed lines. The same color corresponds to the same interpolation order.

Conclusion

An adaptation procedure to generate anisotropic mesh with P_k interpolation has been introduced. It is based on an iterative algorithm to derive a local optimal metric to approximate a given $(k + 1)$ differential form. At each step, a simple linear log-simplex problem is solved in the logarithm space of metric fields . This optimal local metric is then globally optimized *via* a calculus of variations to obtain the optimal distribution of the DoF in $\mathbf{L}^p$ norm. This strategy
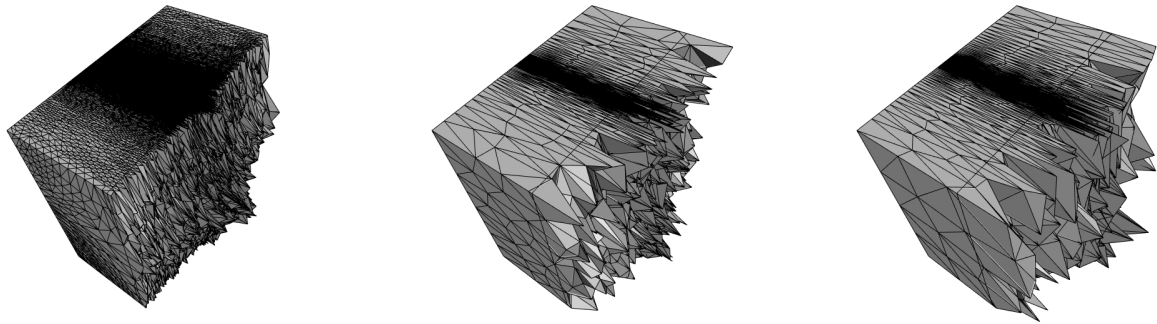
Fig. 10. P_1, P_3 and P_4 adapted meshes for f_s function for the same level of DoF.

has been tested on various 3D examples where the optimal rate of convergence expected from (12) was exhibited. For all the adaptive cases, the adapted meshes have a lower level error and reach faster the asymptotic rate of convergence.

The current work is directed at (i) extending this strategy to $h - p$ adaptation and (ii) coupling this strategy with automatic shock detection for solution involving both smooth and sharp features. The current procedure can take as an input curved meshes as this consists in adding the element mapping in the procedure to compute the $k + 1$ derivative. Consequently, the only limitation to employ curved meshes is in the mesh generation phase. This crucial point is currently investigated.

References

[1] Houman Borouchaki and Paul Louis George. Métriques d'interpolation. *To appear in CRAS*.

[2] Weiming Cao. An interpolation error estimate on anisotropic meshes in $\mathbb{R}^n$ and optimal metrics for mesh refinement. *SIAM J. Numer. Anal.*, 45(6):2368–2391 (electronic), 2007.

[3] Weiming Cao. An interpolation error estimate in $\mathbb{R}^2$ based on the anisotropic measures of higher order derivatives. *Math. Comp.*, 77(261):265–286 (electronic), 2008.

[4] Philippe G. Ciarlet. *The finite element method for elliptic problems*, volume 40 of *Classics in Applied Mathematics*. SIAM, Philadelphia, PA, 2002.

[5] George B. Dantzig and Mukund N. Thapa. *Linear Programming 2: Theory and Extensions*. Springer-Verlag, 2003.

[6] Vít Dolejší. Anisotropic hp-adaptive method based on interpolation error estimates in the L^q-norm. *Applied Numerical Mathematics*, 82:80 – 114, 2014.

[7] Vít Dolejší. Anisotropic hp-adaptive discontinuous Galerkin method for the numerical solution of time dependent PDEs. *Applied Mathematics and Computation*, 267:682 – 697, 2015. The Fourth European Seminar on Computing (ESCO 2014).

[8] Pascal Frey and Paul Louis George. *Mesh generation. Application to finite elements*. ISTE Ltd and John Wiley & Sons, 2nd edition, 2008.

[9] Frédéric Hecht and Raphaël Kuate. An approximation of anisotropic metrics from higher order interpolation error for triangular mesh adaptation. *J. Comput. Appl. Math.*, 258:99–115, 2014.

[10] Adrien Loseille and Frédéric Alauzet. Continuous mesh framework part I: well-posed continuous interpolation error. *SIAM J. Numer. Anal.*, 49(1):38–60, 2011.

[11] Adrien Loseille and Frédéric Alauzet. Continuous mesh framework part II: validations and applications. *SIAM J. Numer. Anal.*, 49(1):61–86, 2011.

[12] Adrien Loseille and Victorien Menier. Serial and parallel mesh modification through a unique cavity-based primitive. In Xiangmin Jiao and Jean-Christophe Weill, editors, *Proceedings of the 22nd International Meshing Roundtable*, 2013.

[13] Jean-Marie Mirebeau. Optimal meshes for finite elements of arbitrary order. *Constructive Approximation*, 32(2):339–383, 2010.

[14] Doug Pagnutti and Carl Ollivier-Gooch. A generalized framework for high order anisotropic mesh adaptation. *Computers & Structures*, 87(1112):670 – 679, 2009. Fifth MIT Conference on Computational Fluid and Solid Mechanics.

[15] M.-G. Vallet, C.-M. Manole, J. Dompierre, S. Dufour, and F. Guibault. Numerical comparison of some Hessian recovery techniques. *International Journal for Numerical Methods in Engineering*, 72:987–1007, 2007.

[16] Masayuki Yano and David L. Darmofal. An optimization-based framework for anisotropic simplex mesh adaptation. *Journal of Computational Physics*, 231(22):7626 – 7649, 2012.